J Biol Inorg Chem
DOI 10.1007/s00775-014-1127-4

ORIGINAL PAPER

Cognate and noncognate metal ion coordination in metal-specific metallothioneins: the *Helix pomatia* system as a model

Òscar Palacios · Sílvia Pérez-Rafael · Ayelen Pagani · Reinhard Dallinger · Sílvia Atrian · Mercè Capdevila

Received: 29 October 2013 / Accepted: 10 March 2014

Abstract The *Helix pomatia* metallothionein (MT) system, namely, its two highly specific forms, HpCdMT and HpCuMT, has offered once again an optimum model to study metal–protein specificity. The present work investigates the most unexplored aspect of the coordination behavior of MT polypeptides with respect to either cognate or noncognate metal ions, as opposed to the standard studies of cognate metal ion coordination. To this end, we analyzed the in vivo synthesis of the corresponding complexes with their noncognate metals, and we performed a detailed spectroscopic and spectrometric study of the Zn^{2+}/Cd^{2+} and Zn^{2+}/Cu^{+} in vitro replacement reactions on the initial Zn-HpMT species. An HpCuMTAla site-directed mutant, exhibiting differential Cu^{+}-binding abilities in vivo, was also included in this study. We demonstrate that when an MT binds its cognate metal, it yields well-folded complexes of limited stoichiometry, representative of minimal-energy conformations. In contrast, the incorporation of noncognate metal ions is better attributed to an unspecific reaction of cysteinic thiolate groups with metal ions, which is dependent on their concentration in the surrounding milieu, where no minimal-energy structure is reached, and otherwise, the MT peptide acts as a multidentate ligand that will bind metal ions until its capacity has been saturated. Additionally, we suggest that previous binding of an MT polypeptide with its noncognate metal ion (e.g., binding of Zn^{2+} to the HpCuMT isoform) may preclude the correct folding of the complex with its cognate metal ion.

Keywords *Helix pomatia* · Metallothionein · Cu-specific · Cd-specific

Electronic supplementary material The online version of this article (doi:10.1007/s00775-014-1127-4) contains supplementary material, which is available to authorized users.

Ò. Palacios · S. Pérez-Rafael · M. Capdevila (✉)
Departament de Química, Facultat de Ciències, Universitat Autònoma de Barcelona, Cerdanyola del Vallès, 08193 Barcelona, Spain
e-mail: merce.capdevila@uab.cat

A. Pagani · S. Atrian
Departament de Genètica, Facultat de Biologia, Universitat de Barcelona, Av. Diagonal 645, 08028 Barcelona, Spain

R. Dallinger
Institute of Zoology, University of Innsbruck, Technikerstraße 25, 6020 Innsbruck, Austria

Introduction

Metallothioneins (MTs) constitute a superfamily of cysteine-rich, low molecular weight proteins with high metal-binding capacity. They are involved in a variety of biological processes, but they are supposed to be mainly responsible for regulating the intracellular levels of biologically essential metal ions (Zn^{2+} and Cu^{+}) and protecting cells from the deleterious effects of toxic metal ions (i.e., Cd^{2+}, Pb^{2+}, Hg^{2+}) [1, 2]. Most organisms contain complex MT systems, composed of homologous proteins that exhibit either similar or highly different binding preferences for divalent versus monovalent metal ions [3]. Although awareness of the molecular basis determining the metal specificity of an MT peptide is fundamental to understand the MT structure–function relationships, their physiological function, and their differentiation pattern through evolution, knowledge of it remains as an unsolved matter.

The best known paradigm of highly similar MT peptides, with fully conserved coordinating Cys residues, but

Published online: 01 April 2014

nevertheless exhibiting opposite metal preferences, is offered by the Roman snail (*Helix pomatia*) MT (HpMT) system [4]. *H. pomatia* encodes three different MT isoforms [5], two of them with highly distinct metal specificities: the Cd-specific (HpCdMT) and the Cu-specific (HpCuMT) isoforms, which share 57 and 73 % sequence identity and similarity, respectively. HpCdMT is apparently involved in Cd binding and detoxification within the digestive tissues of the snail [6], where it is induced specifically in the epithelial cells of gut, midgut gland, and kidney [7]. Contrarily, HpCuMT is expressed in only one cell type (the so-called rhogocytes), where it plays a role in connection with hemocyanin synthesis [8]. The third isoform, denominated HpCdCuMT, confirmed by genomic screening studies [5], does not exhibit any definite metal response patterns and, in fact, never accumulates in any snail tissue [9].

The reports on both native [6–8] and recombinant [5] HpMTs suggest that these two snail MT isoforms achieved their metal-binding specificity by amino acid sequence diversification, which leads the peptide to assume a particular binding configuration that favors metal–MT complex formation with distinct target metal ions. Thus, both HpMT amino acid sequences, despite being highly similar (Table1), show an intrinsic and extremely distinct in vivo metal-binding behavior toward divalent (Zn^{2+} and Cd^{2+}) and monovalent (Cu^{+}) metal ions. Precisely, the recombinant synthesis of both isoforms in *Escherichia coli* allowed reproduction of the behavior and the spectroscopic features observed for these proteins when purified from living organisms [5], and showed how the synthesis of each MT as a complex with its cognate metals renders unique, well-folded complexes, whereas the opposite situation, i.e., the synthesis of noncognate metal complexes, produces a mixture of multiple, ill-defined species. More recently, the role of the unique His residue of the HpCuMT isoform has also been studied through the determination of the in vivo metal-binding properties of the site-directed mutant HpCuMTAla, where His was replaced by Ala (Table 1) [10]. Therefore, once it had been established that the biological basis of the metal specificity in the HpMT system lay in the properties conferred by the amino acid sequence of each isoform [5] and not in other circumstantial events, such as metal availability or gene expression regulation, we planned to analyze the phenomenon of metal specificity from a more chemical point of view. To this end, we investigated in detail the metal-binding properties of the two HpMT isoforms in order to obtain further information about the folding and stability of cognate metal–MT complexes and noncognate metal–MT complexes. First, we analyzed the in vivo synthesis of the HpMT complexes with their noncognate metals, in contrast to the synthesis of the reported cognate metal–MT species [5]. Second, we performed a detailed study of the Zn^{2+}/Cd^{2+} and Zn^{2+}/Cu^{+} in vitro replacement reactions on Zn–HpCdMT, Zn–HpCuMT, and Zn–HpCuMTAla. Overall, the results provide evidence that both proteins bind Cd^{2+} and Cu^{+} differently, and that the species formed with a noncognate metal ion are dependent on the concentration of the metal ions in solution, rather than on the formation of stable, low-energy metal–MT complexes that exhibit a definite stoichiometry. The behavior of these MT peptides with regard to their noncognate metals resembles that of an undefined multidentate ligand, quite far away from the folding and stoichiometric specificity shown when MTs coordinate their cognate metal ions.

Materials and methods

Analytical characterization of recombinantly synthesized and in vitro prepared metal–HpMT preparations

The recombinant constructs and the procedures allowing synthesis and purification of the metal (Zn^{2+}, Cd^{2+}, or Cu^{+}) complexes of the three HpMT isoforms analyzed in this work (HpCdMT, HpCuMT, and HpCuMTAla) have been described elsewhere [5, 10]. The recombinantly (i.e., in vivo) synthesized metal–HpMT preparations were analyzed for element composition (S, Zn, Cd, and Cu) by inductively coupled plasma (ICP) atomic emission spectroscopy (AES) using a Polyscan 61E spectrometer (Thermo Jarrell Ash, Franklin, MA, USA) at appropriate

Table 1 Sequence alignment (ClustalW2) of the recombinant proteins studied in this work: HpCdMT, HpCuMT, and the HpCuMTAla mutant of the latter (His40Ala)

HpCdMT	*G*SGKGKGEK**C**TSA**C**RSEP**C**Q**C**GSK**C**Q**C**GEG**C**T**C**AA**C**KT**C**N**C**TSDG**C**K**C**GKE**C**TGPDS**C**K**C**GSS**C**S**C**K
HpCdCuMT	-SGKGS--N**C**AGS**C**NSNP**C**S**C**GDD**C**K**C**GAG**C**S**C**VQ**C**HS**C**Q**C**NNDT**C**K**C**GNQ**C**SASGS**C**K**C**GS-**C**G**C**K
HpCuMT	*GS*..GRGKN**C**GGA**C**NSNP**C**S**C**GND**C**K**C**GAG**C**N**C**DR**C**SS**C**HC**S**NDD**C**K**C**GSQ**C**TGSGS**C**K**C**GSA**C**G**C**K
HpCuMTAla	*GS*..GRGKN**C**GGA**C**NSNP**C**S**C**GND**C**K**C**GAG**C**N**C**DR**C**SS**C***A***C**SNDD**C**K**C**GSQ**C**TGSGS**C**K**C**GSA**C**G**C**K

The sequence deduced for the native HpCdCuMT isoform is also included. The Cys residues are in bold, and the initial Gly, which is a result of recombinant synthesis, is in italics

wavelengths (S, 182.040 nm; Zn, 213.856 nm; Cd, 228.802 nm; Cu, 324.803 nm) either under "conventional" [dilution with 2 % HNO_3 (v/v)] [11] or under "acidic" (incubation in 1 M HCl at 65 °C for 5 min) [12] conditions. The MT concentration in the recombinant preparations was calculated from the acidic ICP S measurements, assuming the only contribution to their S content was that from the HpMT peptides. Protein concentrations were confirmed by standard amino acid analysis performed with an Alpha Plus amino acid autoanalyzer (Pharmacia LKB Biotechnology, Uppsala, Sweden) after sample hydrolysis in 6 M HCl (22 h at 110 °C). Ser, Lys, and Gly contents were used to extrapolate sample concentrations.

The so-called in vitro complexes were obtained by metal displacement reactions on the recombinant Zn–HpMT preparations, by adding aliquots of standard solutions of the corresponding metal ions (Cd^{2+} or Cu^{+}) to the sample at equivalent molar ratios. Titrations were performed at pH 7.0 following the procedures described elsewhere [13, 14]. All assays were conducted under an Ar atmosphere, and the pH for all experiments remained constant throughout, without the addition of any extra buffers. The in vitro acidification/reneutralization experiments were performed by adapting the procedure reported in [15]. Essentially, 10–20 μM preparations of the in vivo synthesized Cd–HpMTs were acidified from neutral pH (7.0) to acidic pH (1.0) with HCl, kept at pH 1.0 for 20 min, and further reneutralized to pH 7.0 with NaOH. Circular dichroism (CD) and UV–vis spectra were recorded at different pHs during the acidification/reneutralization procedure, both immediately after acid or base addition and 10 min later, always with identical results. During all experiments, strict O_2-free conditions were kept by saturation of all the solutions with Ar.

Spectroscopic and spectrometric characterization of the recombinantly synthesized and the in vitro prepared metal–HpMT preparations

CD spectroscopy was performed using a model J-715 spectropolarimeter (JASCO, Groß-Umstadt, Germany) equipped with a computer (J-700 software, JASCO). Measurements were conducted at a constant temperature of 25 °C, maintained by a Peltier PTC-351 S apparatus (TE Technology, Traverse City, MI, USA). Electronic absorption was measured with an HP-8453 diode-array UV–vis spectrophotometer (GMI, Ramsey, MN, USA), using 1-cm capped quartz cuvettes, and correcting for the dilution effects by means of GRAMS 32 (Thermo Fisher Scientific, Waltham, MA, USA).

Molecular mass determination was performed by electrospray ionization mass spectrometry (ESI-MS) with a time-of-flight analyzer using a micrOTOF-Q instrument (Brucker Daltonics, Bremen, Germany) calibrated with ESI-L low concentration tuning mix (Agilent Technologies), interfaced with a series 1100 high-performance liquid chromatography pump (Agilent Technologies, Santa Clara, CA, USA) equipped with an autosampler, both controlled by Compass. The proteins with divalent metals (Zn, Cd) were analyzed by injecting 20 μL of the sample through a long PEEK tube (1.5 m × 0.18-mm inner diameter) at 40 μL/min under the following conditions: capillary–counter electrode voltage, 5.0 kV; desolvation temperature, 90–110 °C; drying gas 6 L/min. Spectra were collected throughout an *m*/*z* range from 800 to 2,000. The proteins that contain Cu were analyzed by injecting 20 μL of the sample at 30 μL/min under the following conditions: capillary–counter electrode voltage, 4.0 kV; desolvation temperature, 80 °C; *m*/*z* range from 800 to 2,000. The liquid carrier was a 90:10 mixture of 15 mM ammonium acetate and acetonitrile, pH 7.0. For the analysis at acidic pH, the conditions used were the same as those used in the analysis in the case of divalent metals, except for the composition of carrier liquid, which in this case was a 95:5 mixture of formic acid and acetonitrile at pH 2.4. The composition of the complexes synthesized in Cu-enriched cultures was routinely analyzed by ESI-MS at two pH values, 7.0 and 2.4, since Cu(I)–thiolate, but not Zn(II)–thiolate bonds persist at pH 2.4, whereas at pH 7.0 both metal ions are indiscernible owing to the closeness of their atomic masses. All the samples were injected at least in duplicate to ensure reproducibility. In all cases, molecular masses were calculated according to the method reported in [16].

Results and discussion

Zn^{2+} binding to the HpMT isoforms

The recombinant synthesis of HpCdMT by Zn-supplemented *E. coli* cells rendered the canonical Zn_6–HpCdMT complex as a single, well-defined species, according to its preference for divalent metal ion binding, as extensively discussed in [5]. In contrast, the Zn–HpCuMT and the Zn–HpCuMTAla preparations obtained under equivalent conditions showed all the distinctive characteristics of non-cognate metal ion binding [17]. Hence, the synthesis of HpCuMT in Zn-rich cultures invariably yielded a mixture of Zn–MT species of different stoichiometry, whose relative proportion differed in the different preparations. The corresponding ESI-MS analysis showed that the major species ranged from Zn_5–HpCuMT to Zn_7–HpCuMT (Fig. 1a–c), which is in accordance with the Zn_5– and Zn_6–HpCuMTAla almost equimolar composition reported for the mutated HpCuMTAla form [10]. All the Zn–HpCuMT

preparations exhibited equivalent CD spectra, showing the typical profiles of the Zn–MT complexes centered at 240 nm, although with a very low intensity that suggested a poor degree of folding of the corresponding Zn complexes when compared with those rendered by HpCdMT (Fig. 1d).

Cd^{2+} binding to the HpMT isoforms

In vivo synthesis of Cd–HpMT complexes

As shown in [5], the recombinant synthesis of HpCdMT in Cd^{2+}-rich medium rendered the expected single Cd_6–HpCdMT species, which exhibited a CD profile that perfectly matches that previously recorded and extensively analyzed for the native Cd_6–HpCdMT species [18]. Therefore, the behavior of an MT peptide when binding its cognate metal ion is also perfectly illustrated in this case (see Fig. 2d).

Contrarily, and coincidently with the data presented earlier for Zn^{2+} binding, variable results were obtained for the preparations of HpCuMT, and also of HpCuMTAla [10], obtained from Cd^{2+}-enriched bacterial cultures. The Cd–HpCuMT preparations have been grouped in three different types (types 1–3), depending on the major species found by their respective ESI-MS analysis (Fig. 2a). In all three cases, the presence of sulfide-containing species, Cd_xS–HpCuMT, was clearly evident [12], this being totally concordant with the peculiarities of Cd^{2+} binding by a copper thionein [17]. The CD spectra of the three types of preparations differ from one another, as a result of their different compositions, and significantly, they also diverge from the spectrum expected for the conventional Cd–MT species reported in the literature (Fig. 2b) [12]. As common traits, they exhibit the absorptions of the Cd–SCys chromophores clearly detectable at approximately 250 nm, appearing as Gaussian bands in types 1 and 2, and the signals at about 280 nm related to the presence of Cd–sulfide bonds, which are more clearly defined in type 3, in accordance with the abundance of the Cd_9S–HpCuMT species. It is worth noting that the Cd–HpCuMT preparations showed another typical behavior of the Cd^{2+} complexes formed by copper thioneins, which is the variation of their CD profiles with time, firstly identified and reported for the paradigmatic yeast Cup1 MT [19]. The three types of Cd–HpCuMT preparations evolved during a period up to 20 days, and yielded samples richer in the sulfide-containing species to the detriment of the canonical Cd_6–HpCuMT, Cd_7–HpCuMT, and Cd_8–HpCuMT complexes. These variations in composition are accompanied by changes in the UV–vis and CD spectra that support the hypothesis of important alterations of the coordination environments about the Cd^{2+} ions (unpublished results).

The recombinant synthesis of HpCuMTAla in Cd^{2+}-enriched medium [10] gave rise to results equivalent to those described for type 3 HpCuMT preparations, revealing that the His residue does not play a major role in divalent metal ion binding.

In vitro formation of Cd–HpMT complexes

To deepen our understanding of the different Cd-binding behavior of both HpMT isoforms, two sets of in vitro experiments were performed: the Zn/Cd displacement reaction on the recombinant Zn–HpMTs; and the denaturation/refolding of the recombinant Cd–HpMT complexes. For the sake of brevity, not all experimental data are shown, but the corresponding results are described in the following sections.

HpCdMT The displacement of Zn^{2+} by Cd^{2+} in Zn_6–HpCdMT was a straight reaction that yielded Cd_6–HpCdMT after the addition of 6 Cd^{2+} eq (Fig. 3e), coincidently with the result of the in vitro reconstitution of Cd–HpCdMT complexes from apo forms obtained from native material [18]. Analysis of the progressive stages of this reaction revealed that Zn^{2+} is replaced by Cd^{2+} one for one, this yielding the formation of a mixture of Zn_xCd_y–HpCdMT complexes, where $x + y = 6$ (Fig. 3d), following a pattern (Fig. 3a, b) similar to that described for Cd^{2+} binding to the mammalian Zn_7–MT1 [20, 21]. Further additions of Cd^{2+} provoke only small structural reorganizations of the Cd_6–HpCdMT species (Fig. 3c), but with no further incorporation of Cd^{2+} ions, as shown by the minor changes in the UV–vis (data not shown) and ESI-MS (Fig. 3f) spectra. Denaturation/renaturation of recombinant Cd_6–HpCdMT allowed recovery of the initial species (Fig. 3c). Therefore, both types of experiments rendered in-vitro-constituted Cd_6–HpCdMT species with spectroscopic (Fig. 3c) and spectrometric (Fig. 3e) features analogous to those of recombinantly synthesized [5] or natively purified [18] species. Overall, this indicates that HpCdMT achieves a unique folding about Cd^{2+} both in vivo (native and recombinant) and in vitro (Cd^{2+} titration of Zn–HpCdMT and renaturation of Cd–HpCdMT), a behavior assignable to an MT optimal for Cd^{2+} binding [17], in contrast with the behavior observed for the Cd–MT complexes of other mollusk MTs, such as the mussel MT10-IV isoform [22], that exhibit better coordination abilities toward Zn^{2+} than toward Cd^{2+}.

HpCuMT In vitro experiments parallel to those described in the previous section were performed with Zn–HpCuMT and Zn–HpCuMTAla, with equivalent results for both HpCuMT peptides. Although in this case the starting point of each Cd^{2+} titration was a mixture of several Zn–HpMT

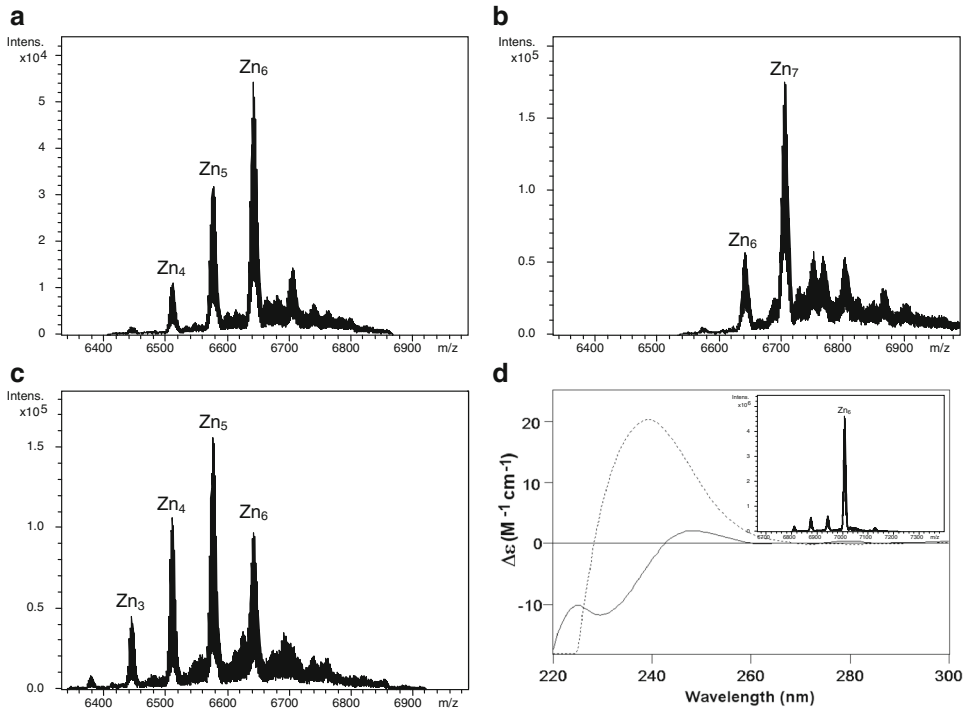

Fig. 1 **a–c** Deconvoluted electrospray ionization mass spectrometry (ESI-MS) spectra corresponding to different syntheses of HpCuMT in Zn^{2+}-enriched bacterial cultures. **d** Characteristic circular dichroism (CD) spectra of the Zn–HpCuMT preparations (*solid line*) and the Zn–HpCdMT preparations (*dotted line*). The *inset* shows the ESI-MS spectrum of Zn–HpCdMT [5]

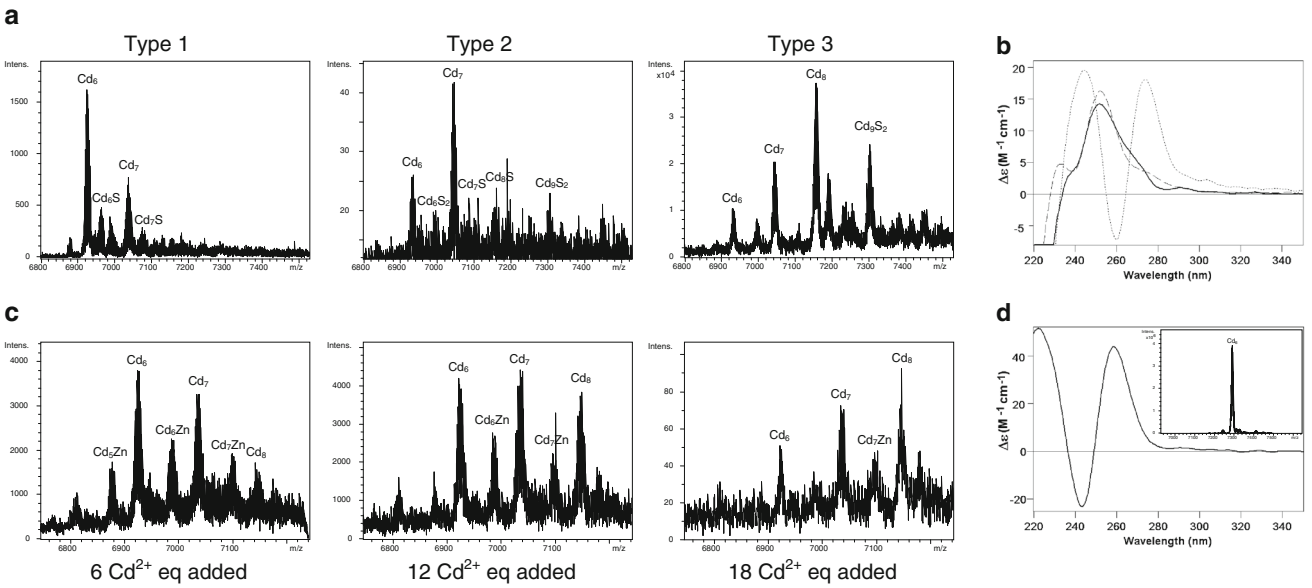

Fig. 2 **a** Deconvoluted ESI-MS spectra corresponding to the three types of Cd–HpCuMT preparations. **b** CD spectra of type 1 (*solid line*), type 2 (*dashed line*), and type 3 (*dotted line*) Cd–HpCuMT preparations. **c** Deconvoluted ESI-MS spectra recorded at different steps of the titration of Zn–HpCuMT with Cd^{2+}. **d** CD and ESI-MS spectra corresponding to the Cd–HpCdMT preparation [5]

species (see Fig. 1), it was always still possible to spectroscopically and spectrometrically follow the progression of the reaction (full data in Figs. S1 and S2 for Zn–HpCuMTAla). It became readily evident that the multiplicity of species recovered from the recombinant Cd–HpCuMT synthesis is a manifestation of the profusion of the metal complexes that are formed during the Zn/Cd replacement reaction. In fact, at distinct stages of the Cd^{2+} titration of Zn–HpCuMT, the speciation of each of the three different Cd–HpCuMT preparations could be almost achieved except, obviously, for the sulfide-containing species (Fig. 2c). However, it is interesting to note that even with a clear Cd^{2+} excess (16 Cd^{2+} eq added to Zn–HpCuMTAla), Zn^{2+}-containing species remained in

solution, which only disappeared on S^{2-} addition, allowing the formation of the corresponding sulfide-containing complexes (Fig. S2). This is indicative of the nonoptimal capacity of the HpCuMT polypeptide to cope with Cd^{2+} ions, resulting in the requirement of additional elements, either residual Zn^{2+} ions or S^{2-} anions, to maintain a subpopulation of metal complexes [17].

Finally, the denaturation/renaturation process of any of the recombinant Cd–HpCuMT preparations rendered a unique CD envelope similar to that corresponding to the final step of the Cd^{2+} titration (Fig. S1) and obviously not coincident with that of any of the three types of recombinant syntheses (see Figs. 2, S1) as a result of the absence of S^{2-}-containing species.

It is remarkable that at high Cd^{2+} concentrations, highly nucleated species, exceeding the canonical M_6 content, are formed: Cd_7, Cd_8, and even Cd_9S. These complexes are still affordable, since the 18 Cys of the polypeptide can theoretically contribute up to 36 thiolate bonds (as bridging Cys), enough for the tetrahedral coordination of up to nine Cd^{2+} ions. Nevertheless, it is striking that unlike HpCuMT, the HpCdMT isoform, with the same number of Cys residues, never exceeds the Cd_6 stoichiometry, which would correspond to an extremely stable conformation trapped in a final energy well [5]. Therefore, overall, the data indicate that when binding Cd^{2+}, the HpCuMT polypeptide is far from attaining a single energetically favored conformation, behaving instead like a multidentate ligand that just responds to the increase in Cd^{2+} ions in media under both in vivo and in vitro conditions.

Cu^+ binding to the HpMT isoforms

In vivo synthesis of Cu–HpMT complexes

The recombinant synthesis of Cu^+–HpMT complexes in Cu-enriched cells yielded much more definite results for the HpCuMT isoform (i.e., cognate pair) than for the HpCdMT peptide, similarly to the results observed for the Cd^{2+}/HpCdMT combination. We have previously shown that low aeration of the producing *E. coli* cultures implies high Cu concentrations in the growing bacteria [23]. Hence, the HpCuMT peptide produced in low-aerated Cu-supplemented cultures yielded a major homometallic Cu_{12}–HpCuMT complex [5], together with some very minor Cu_{13} complexes, coincidently again with previous native sample characterization [24] (Fig. 4). It is worth noting that the analysis of the same sample under neutral and acidic ESI-MS conditions produced different results: Cu_{12}–HpCuMT and Cu_{10}–HpCuMT, respectively (Fig. 4a), which indicates that the canonical Cu_{12}–HpCuMT species would be constituted by a highly stable Cu_{10} cluster plus two Cu^+ ions more loosely bound. Instability of some Cu^+ ions in the Cu–MT complexes detected by acidic ESI-MS analysis has been reported before [25]. Normally aerated cultures yielded a preparation with equimolar Zn and Cu contents, containing a mixture of Cu,Zn–HpCuMT species ranging from M_4–HpCuMT to M_{12}–HpCuMT (M is Zn and Cu) (Fig. 4a). The CD fingerprints of both preparations differed notably, in accordance with the presence of homonuclear versus heteronuclear complexes, but both showed absorptions in the 250–300-nm range. Clearly the production at low aeration resulted in higher-intensity and better defined CD bands (Fig. 4b). The synthesis of the HpCuMTAla mutant in Cu-enriched media produced similar results, but pointing at a higher Cu-binding ability. Thus, normally aerated cultures allowed the recovery of heteronuclear Cu,Zn–HpCuMTAla species but with a higher Cu^+ content than for the wild-type form (seven Cu to three Zn, according to the ICP-AES results), and the homonuclear Cu_{12}–HpCuMTAla complexes obtained at low aeration exhibited a higher relative stability than Cu_{12}–HpCuMT. As discussed before [10], these results indicate that the presence of His in HpCuMT decreases the Cu-binding abilities of this isoform in relation to those of the His/Ala-substituted mutant. This suggests that the presence of His in HpCuMT could confer on it optimal combined abilities both for Cu binding and for Cu release. Such a plasticity would be essential for a putative role of HpCuMT in the transfer of Cu(I) to biomolecules that require it, as repeatedly hypothesized for hemocyanin synthesis in snail roghocytes.

The behavior of an MT peptide toward its noncognate metal was evidenced once again when we characterized the synthesis of HpCdMT in Cu-rich medium, because this rendered mixtures of heterometallic Cu_xZn_y–HpCdMT complexes both in regularly aerated and in low-aerated cultures. Obviously, the Zn content of the preparations was higher in the former than in the latter (three Zn to two Cu vs one Zn to eight Cu, respectively). Under normal aeration, the species recovered ranged from M_3–HpCdMT to M_8–HpCdMT, with M_5–HpCdMT and M_4–HpCdMT as the most abundant species, whereas in low-aerated cultures, complexes ranging from M_8–HpCdMT to M_{12}–HpCdMT (M is Zn and Cu) were obtained (Fig. 5a). Acid–ESI-MS spectra showed that this isoform was able to render almost unique Cu_4 clusters in regular intracellular Cu concentrations (i.e., normal aeration) and a mixture of Cu_8 to Cu_{11} clusters, with major Cu_8 clusters, under high Cu (Fig. 5a). Both preparations gave rise to comparable CD signals, both in shape and in intensity, although the fingerprint of the preparations under normal aeration exhibited wider and less defined bands than those corresponding to low-aerated cultures (Fig. 5b). Finally, the detection of an important amount of apo-HpCdMT in the acidic ESI-MS analyses of Cu–HpCdMT produced under regular aeration suggested that under this condition, and

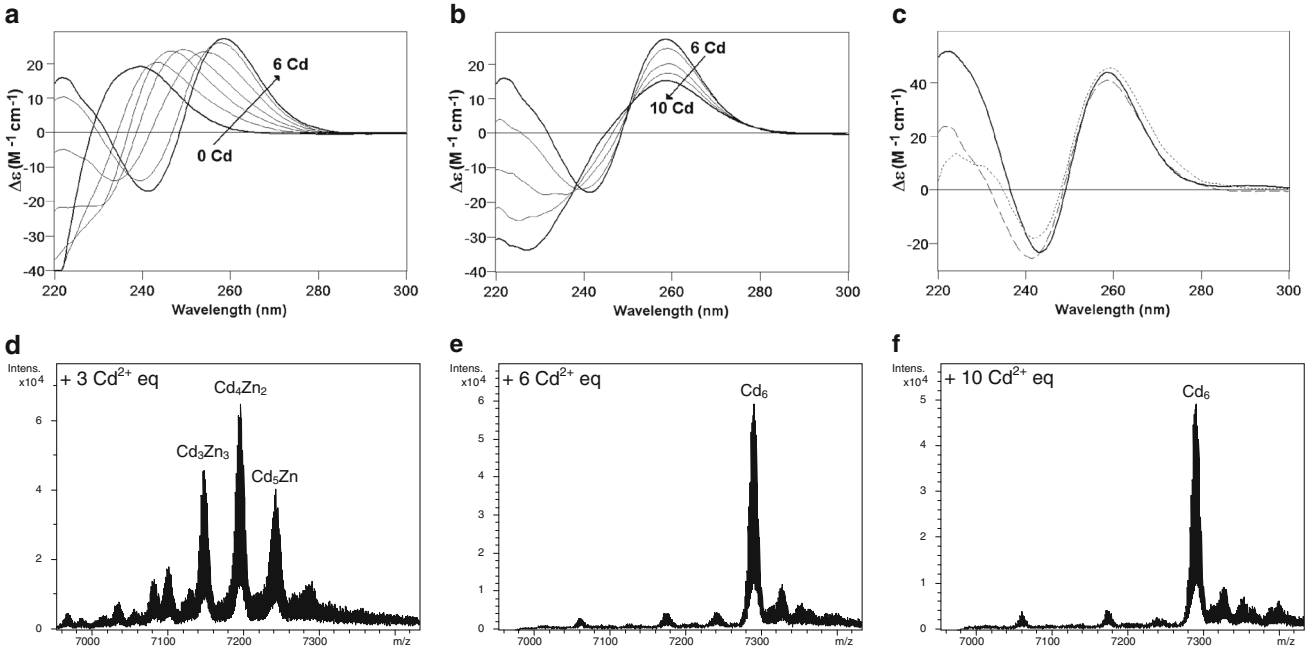

Fig. 3 **a**, **b** CD spectra and **d**–**f** deconvoluted ESI-MS spectra corresponding to different steps of a titration of a 15 μM solution of Zn_6–HpCdMT with Cd^{2+} at pH 7.0. **c** Comparison of the normalized CD fingerprints of the Cd_6–HpCdMT preparations obtained recombinantly (*solid line*), by Zn/Cd displacement on Zn–HpCdMT (*dashed line*), and by denaturation/renaturation of Cd–HpCdMT (*dotted line*)

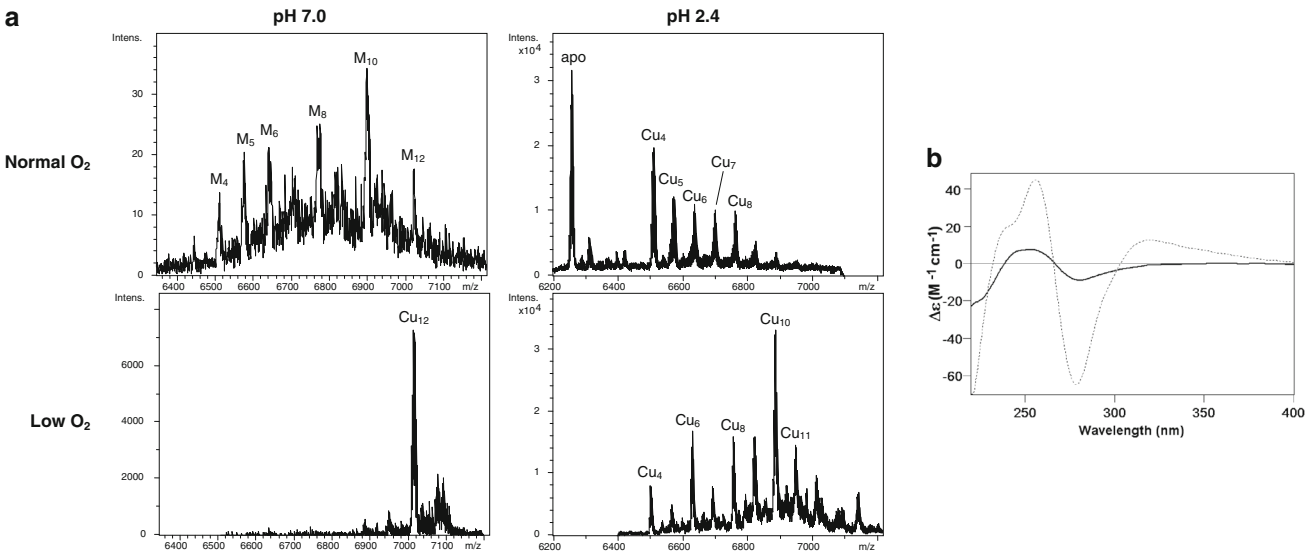

Fig. 4 **a** Deconvoluted ESI-MS spectra of the recombinant preparations of HpCuMT in Cu^{2+}-enriched medium under normal-aeration or low-aeration conditions at pH 7.0 and pH 2.4. *M* represents Zn and Cu, owing to the difficulties in ESI-MS to discriminate between these two metal ions. **b** CD spectra corresponding to the preparations of Cu–HpCuMT under normal-aeration (*solid line*) and low-aeration (*dotted line*) conditions, recorded at pH 7.0

despite the supplementation of the bacterial culture with Cu salts, the synthesis of the peptide gave rise either to major Zn–HpCdMT species or to rather unstable Cu_4 cores, both possibilities compatible with the intrinsic poor ability of HpCdMT to bind Cu^+.

In vitro formation of Cu–HpMT complexes

By HpCuMT Further in vitro experiments were undertaken to deepen our knowledge of the differential Cu^+-binding abilities of the genuine copper thionein HpCuMT.

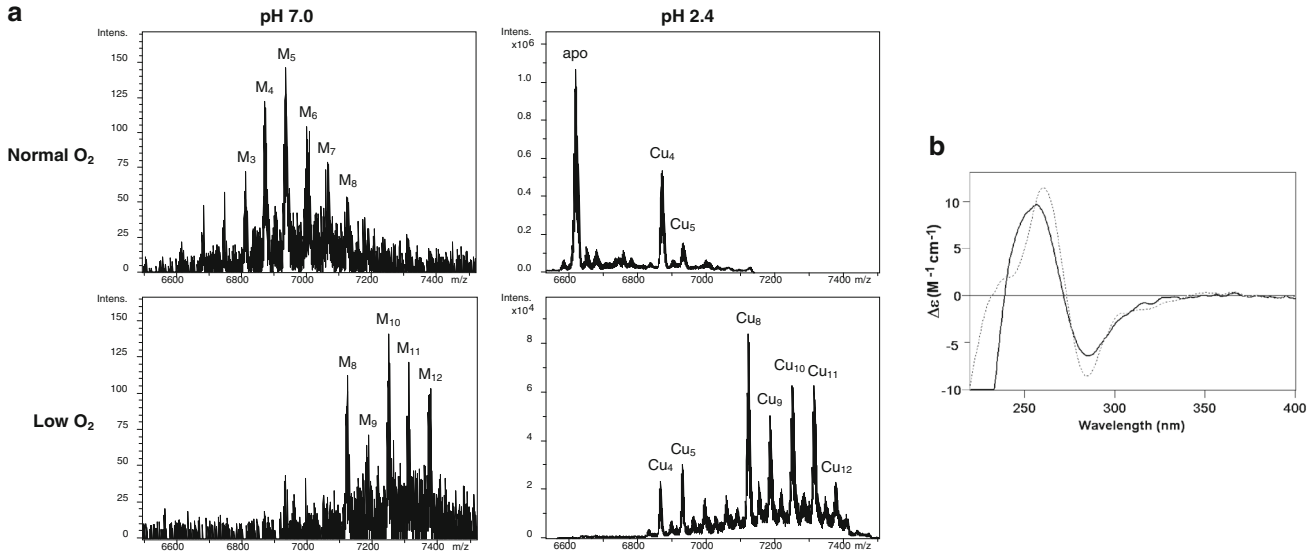

Fig. 5 **a** Deconvoluted ESI-MS spectra of the recombinant preparations of HpCdMT in Cu^{2+}-enriched medium under normal-aeration or low-aeration conditions at pH 7.0 and pH 2.4. *M* represents for Zn and Cu, owing to the difficulties in ESI-MS to discriminate between these two metal ions. **b** CD spectra corresponding to the preparations of Cu–HpCdMT under normal-aeration (*solid line*) and low-aeration (*dotted line*) conditions, recorded at pH 7.0

Precisely, the Cu-binding features of two distinct starting samples were analyzed: (1) recombinant Zn–HpCuMT; and (2) the recombinant Zn,Cu–HpCuMT mixed complexes obtained from regularly aerated cultures (see Fig. 5a). The Cu^+ titration of Zn–HpCuMT (experiment 1) always rendered mixtures of heteronuclear Zn,Cu–HpCuMT species, of different composition depending on the titration stage considered (Fig. 6c). Unexpectedly, the interaction of Cu^+ with the Zn–HpCuMT complexes was difficult and slow, and the major complexes obtained were M_8–HpCuMT species containing Cu_4 clusters, even when 12 Cu^+ eq had been added to the reaction mixture. M_{10} was the highest stoichiometry detected, and this species was in an equimolar amount with M_8 when 8 Cu^+ eq had been added to Zn–HpCuMT. Significantly, this stage of the titration rendered the mixture of species closest to that of the in vivo preparation obtained under regular aeration. Beyond this point, more Cu^+ added accounted for the decrease in the amount of the M_{10}–HpCuMT species (Fig. 6c). In experiment 2, when Cu^+ equivalents were progressively added to the heteronuclear Zn,Cu–HpCuMT preparation, the predominant component of the samples obtained at different stages was invariably M_{10}–HpCuMT, followed in abundance by M_8–HpCuMT. But acidic ESI-MS analyses revealed that now these species included Cu_8 and Cu_4 clusters, almost in the same ratio, when 6 Cu^+ eq had been added to the starting solution, and invariably until 12 Cu^+ eq had been added (see Fig. 6c). Notably, at this point, a homonuclear Cu_{10} species was obtained as a major component, together with Cu_8 species and some remaining Zn_xCu_4 species. No further Cu^+ incorporation into these complexes could be achieved when extra Cu^+ equivalents were added (Fig. 6b). Significantly, this homonuclear Cu_{10} species could therefore be representative of the Cu_{10} core of the Cu_{12} species recombinantly obtained under low culture aeration (Fig. 4a).

Therefore, these results indicate that the Zn/Cu exchange in a preformed Zn–HpCuMT complex is unable to yield a Cu–HpCuMT complex analogous to the in-vivo-folded ones, either natively or heterologously, whereas the addition of further Cu to a mixed Zn,Cu complex, folded in the presence of Cu, can render Cu_{10}–HpCuMT complexes, representative of the core present in Cu_{12}–HpCuMT. The comparison of the CD spectra of the different types of samples also highlights that the CD fingerprint of Cu_{12}–HpCuMT is not reproduced by any Cu^+ titration reaction on Zn^{2+}-containing HpCuMT complexes (Fig. 4b vs Fig. 6a, b). From these considerations, it may be concluded that the presence of Zn^{2+} initially bound to HpCuMT, does not preclude the binding of Cu^+, but promotes a particular folding that hampers the incoming Cu^+ ions from achieving the characteristic native stoichiometry and folding. Therefore, the Zn^{2+} coordination exerts a scaffold effect that would be incompatible with homometallic Cu clusters and precisely with the "Cu_{12} architecture". As a result, it is sensible to propose that the synthesis of Cu_{12}–HpCuMT requires an especial cell environment, mainly consisting of high Cu concentration. This complex would be stable only under mild conditions (i.e., neutral pH), and its synthesis would be dependent on the direct incorporation of at least

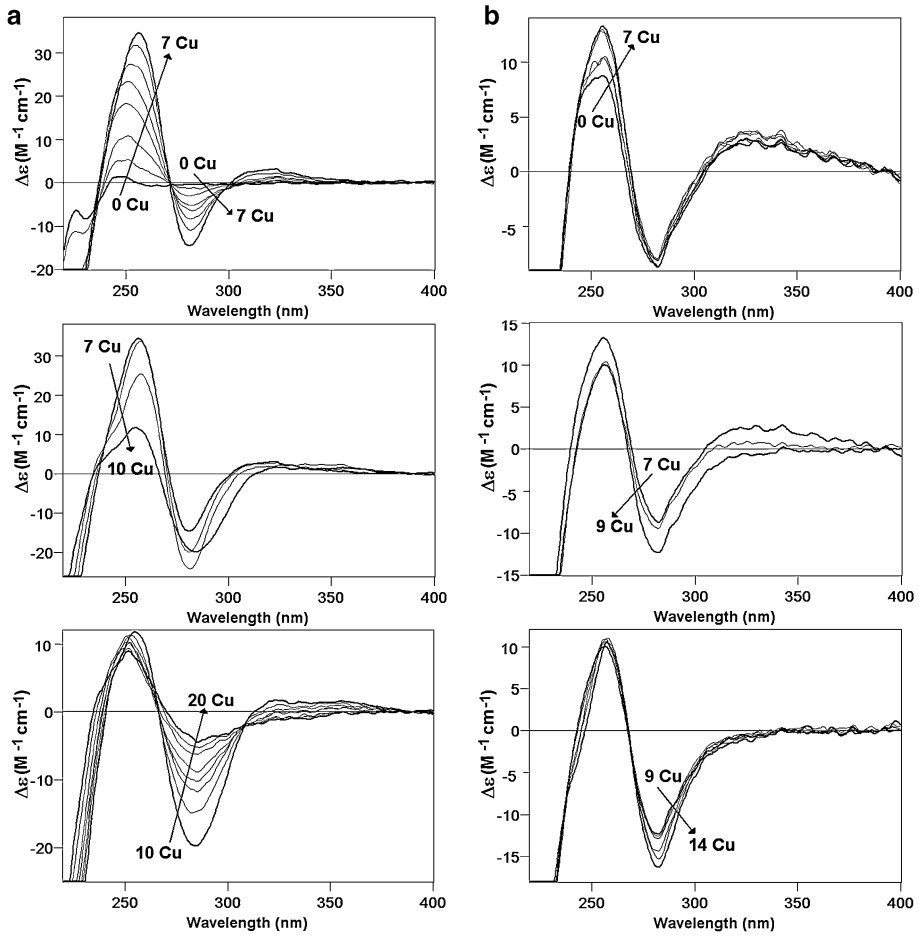

c

Zn-HpCuMT + Cu^+		
Eq.	pH 7.0	pH 2.5
0 Cu	**Zn_6 > Zn_5**	apo
4 Cu	**M_6 > M_7**	apo **> Cu_1 > Cu_4**
5 Cu	**M_8 >> M_9**	apo **> Cu_1 ≈ Cu_4**
7 Cu	**M_8 > M_{10}**	**Cu_4 > Cu_1**
8 Cu	**M_8 ≈ M_{10}**	**Cu_4** > others
10 Cu	**M_8 > M_n**	**Cu_4**
12 Cu	**M_8 >> M_n**	**Cu_4**

Zn,Cu-HpCuMT+ Cu^+		
Eq.	pH 7.0	pH 2.5
0 Cu	**M_{10} > M_8**	apo **> Cu_4**
6 Cu	**M_{10} > M_8**	**Cu_8 ≈ Cu_4**
7 Cu	**M_{10} > M_8**	**Cu_8 ≈ Cu_4**
9 Cu	**M_{10} > M_8**	**Cu_8 ≈ Cu_4**
12 Cu	**M_{10} > M_8**	**Cu_{10} > Cu_8 ≈ Cu_4**

Fig. 6 CD spectra obtained during the titration of 20 μM solutions of **a** Zn–HpCuMT and **b** Zn,Cu–HpCuMT with Cu^+ at neutral pH. **c** The two/three major species detected by ESI-MS at different stages of the previous titrations. *M* stands for Zn and Cu, owing to the difficulties in ESI-MS to discriminate between these two metal ions

some Cu^+ ions, instead of being the product of a total Zn/Cu replacement on Zn–HpCuMT. Unfortunately, the titration of Zn–HpCuMT with Cu^+ at acidic pH, which would have illustrated a de novo folding of HpCuMT about Cu^+, yielded ESI-MS spectra with excessive background noise to be analyzed. But the main conclusion when studying the Cu^+-binding abilities of the HpCuMTAla mutant was that the absence of the His residue present in HpCuMT conferred an unusual stability on the Cu_{12}–HpCuMTAla species over the Cu_{10}–HpCuMTAla core, which was only detected as a second peak in the acidic ESI-MS spectra [10]. This is in agreement with our proposal of the wild-type Cu_{12}–HpCuMT complex enclosing two poorly bound Cu^+ ions, and that the His40 residue is responsible for this.

By HpCdMT The in vitro addition of Cu^+ to Zn_6–HpCdMT (i.e., the titration of a noncognate pair; Figs. 7 and S3) better reproduced the features of the Cu–HpCdMT preparations obtained under low aeration than those of

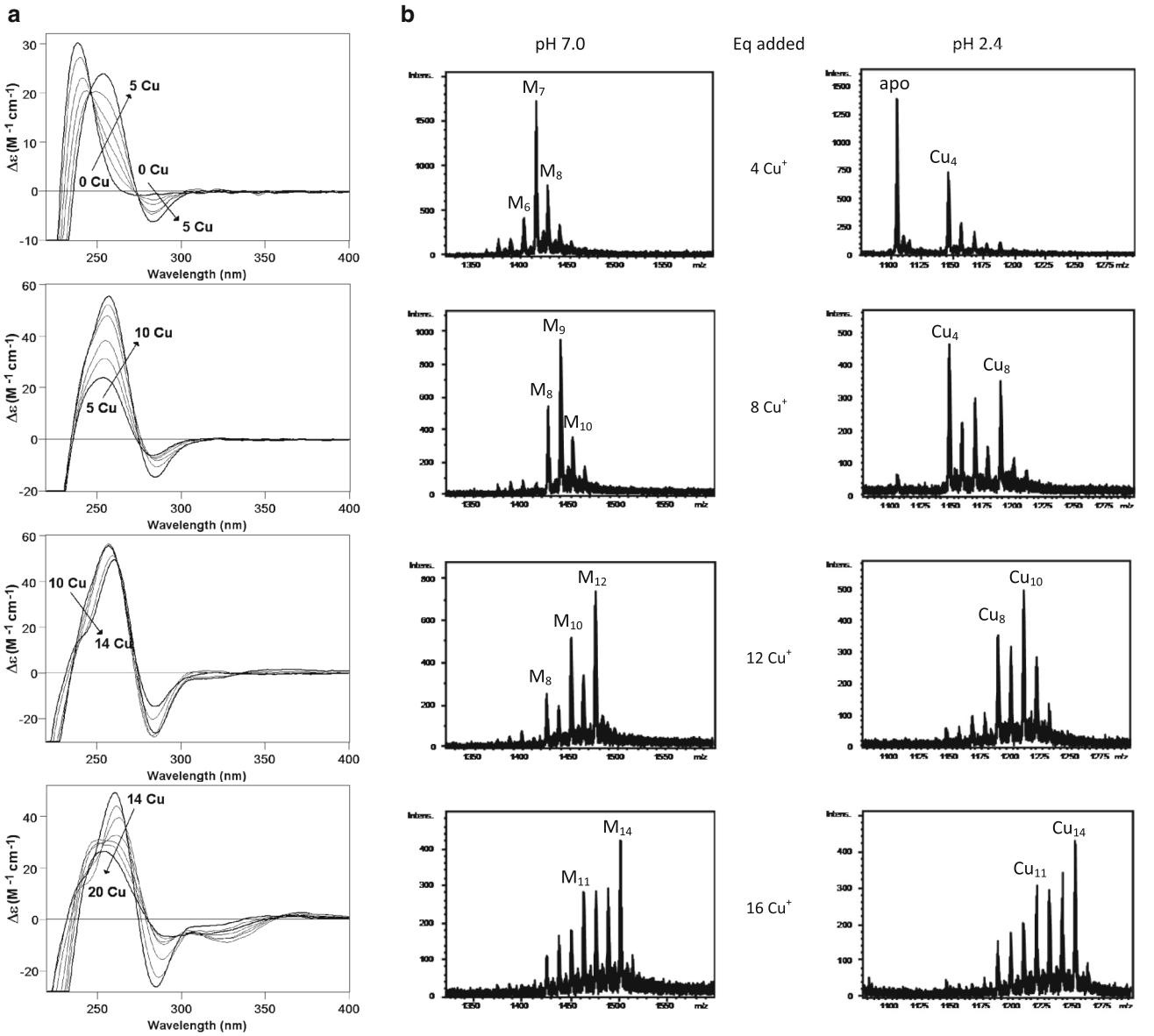

Fig. 7 **a** CD spectra corresponding to the titration of a 20 μM solution of Zn_6–HpCdMT with Cu^+, and **b** selected ESI-MS spectra recorded at different steps of the titration and analyzed at neutral (+5 charge state) and acidic (+6 charge state) pH. The full set of spectra is provided in Fig. S3. *M* stands for Zn and Cu, owing to the difficulties in ESI-MS to discriminate between these two metal ions

cultures under regular aeration. Hence, the data clearly indicate that 16 Cu^+ eq is required to totally displace the Zn^{2+} initially bound to the protein through a noncooperative process, as revealed by the species detected by ESI-MS performed under neutral and acidic conditions. The presence of Cu^+ ions provokes the formation of a predominant Cu_4 cluster and other minor $Cu_{n>4}$ clusters, accompanied by remaining Zn^{2+} ions (M_4 to M_9 species), until 8 Cu^+ eq have been added. At some point before the addition of the 4th Cu^+ equivalent, the speciation of the in vivo sample would be reproduced, since the acidic ESI-MS spectra also reveal a significant presence of apopeptides, corresponding to Zn^{2+}-loaded forms both in vivo (Fig. 5) and in vitro (Figs. 7, S3). Additional Cu^+ added, between 8 and 16 eq, led to higher-nuclearity species, eventually reaching a Cu_{14} maximum stoichiometry, but it is noteworthy that the species present when the 12th Cu^+ eq was added, detected both at neutral and at acidic pH, are those that better reproduce the speciation of Cu–HpCdMT obtained from low-aerated cultures (Figs. 5a, 7b). Beyond this point, additional Cu^+ causes unfolding of the metal complexes, since the total metal content decreases and apopeptides become the main component of the sample, a typical behavior of non-copper thioneins when exposed to excess Cu^+ [26, 27].

The displacement of Zn^{2+} by Cu^{+} in Zn_6–HpCdMT provokes the conventional gradual increase of the UV–vis absorptions at approximately 260 nm until 16 Cu^{+} eq has been added (data not shown). In parallel, the CD envelope of the sample evolves through the different stages of the reaction. Interestingly, when comparing the CD fingerprint and the ESI-MS data of this titration with those of HpCdMT synthesized in Cu-rich medium, under both aeration conditions, we observe that they reproduce more closely the results of the low-O_2 preparation than those of the normal-O_2 preparation. This indicates that, contrarily to what happened with the HpCuMT isoform, the initial folding of HpCdMT with a cognate metal ion, such as Zn^{2+}, does not prevent the Cu–HpCdMT complexes achieving the same final folding either when they are expressed by bacteria or when they are the product of an in vitro Zn/Cu replacement.

Conclusions

All the data presented in this work show that the in vitro metal-binding behavior of both HpMT isoforms, HpCdMT and HpCuMT, illustrates the features reported for their respective recombinant synthesis in metal-supplemented *E. coli* cultures [5, 10], providing further information on the basis of the high coordinative specificity exhibited by HpCdMT for Cd^{2+}, and by HpCuMT for Cu^{+}. Obviously, both isoforms, as all MT peptides, are able to bind both divalent and monovalent metal ions, but the species formed in each case are strongly dependent on the cognate or noncognate nature of the bound metal ion. As a rule of thumb, whereas the coordination of the cognate metals leads to unique, energetically optimized, complexes that define the MT metal specificity, coordination of the noncognate metal ions renders mixtures of complexes, none of them with a conformation compatible with a definite energy well, and thus principally dependent on the amount of metal ions present in solution. Hence, HpCdMT binds up to six Cd^{2+} ions in a very defined and stable folding, yielding Cd_6–HpCdMT species that do not react with excess Cd^{2+}. Contrarily, at high Cd^{2+} concentrations, HpCuMT renders Cd_7, Cd_8, and even Cd_9S species, containing sulfide ligands that exceed the canonical M_6 content. These complexes, which are still affordable when taking into account the number of potential metal–thiolate bonds contributed by the 18 Cys of HpCuMT, suggest that there are different Cd^{2+}–MT connectivity models, all possible but not energetically favored enough. This differential behavior for cognate versus noncognate metal binding has also patently clear consequences in the metal replacement reactions, such that titration with noncognate metals yields less defined folding and stoichiometries than with the corresponding cognate metals. Several examples in the literature nicely illustrate this, both for divalent-metal-preferring MTs (e.g., mammalian MT1 [14, 20, 21, 28] and MT2 [29] and *Caenorhabditis elegans* MT [30]) and for copper thioneins (yeast Cup1 [19], *Drosophila* MtnA [31], and *Cryptococcus neoformans* MT1 and MT2 [25, 32]).

In relation to Cu^{+} binding, it is evident that the presence of Zn^{2+} initially bound to HpCuMT, although not precluding further binding of Cu^{+}, promotes a particular folding that hampers the incoming Cu^{+} ions from achieving the characteristic native Cu_{12}–HpCuMT stoichiometry and folding. Therefore, it has to be assumed that living systems would preclude the formation of initial Zn^{2+} complexes for copper thioneins, to allow these MTs to achieve their proper final fold as homometallic Cu complexes. This may be achieved in two ways. First, by an intrinsic property of the copper thionein polypeptides, which besides providing the capacity of forming stable homonuclear Cu complexes exhibit an inherent difficulty to bind Zn^{2+} at physiological cell concentrations, so that fully metalated Zn^{2+} complexes are never formed under these conditions, as we formerly studied [33]. It was then shown that the recombinant synthesis of MTs in standard (i.e., non-metal-supplemented) medium yielded fully Zn^{2+} loaded complexes in the case of zinc thioneins (e.g., mammalian MT1), but a mixture of apo forms and undermetalated Zn^{2+} complexes in the case of copper thioneins (e.g., *Drosophila* MtnA and MtnB). Second, the compartmentalized expression of this isoform in rhogocytes may further ensure both the absence of basal Zn^{2+} ions and the high Cu^{+} concentrations and the necessary reductive environment for the formation and stability of the Cu^{+}–MT complexes exhibiting their "correct" fold and stoichiometry. Finally, it becomes obvious that the Cu^{+}-binding properties of HpCdMT are rather poor, and that the presence of Cu^{+} ions together with Cd^{2+} ions in the digestive tract of snails, which is the main tissue where this isoform is expressed, would hardly preclude its Cd^{2+} detoxification role.

The analysis of the protein sequences of both isoforms reveals that their different behavior has to be attributed to the different amino acids interspersed between coordinating Cys residues, such as their distinct lateral chain size or/and charge distribution, or Pro situation (Table 1). When we compare the HpCdMT and HpCuMT sequences, it is worth noting that HpCuMT exhibits a higher Gly and Asn content than HpCdMT, whereas HpCdMT is richer in Ser, Thr, and Lys. HpCuMT includes fewer total charged residues than HpCdMT (among the differential residues: three positive and three negative charges in the former vs six positive and four negative charges in the latter). Finally, when we calculate the residue volume (according to [34]), it is obvious

that the HpCdMT isoform is bulkier than HpCuMT (volume increment 421.9 $Å^3$). Pro is another relevant residue that has been suggested to confer some peculiar metal-binding properties on the MT peptides, precisely on mammalian MT3 [35]; however, there is only one position entailing a differential Pro between both snail MT isoforms. Overall, the data suggest a bulkier and more rigid character for HpCdMT and a more flexible nature for the HpCuMT polypeptide, which would confer on the latter a higher coordination versatility to optimally accommodate 12 Cu^+ ions, probably through different coordination geometries. Unfortunately, at present there is no solved 3D structure for any snail metal–MT complex. However, for Cd_6–HpCdMT, several indirect pieces of evidence point to a bidominial folding enclosing two Cd_3Cys_9 clusters. First, spectroscopic data demonstrated that the reconstitution of the Cd_6–HpCdMT complex from Cd^{2+} titration of the corresponding apoprotein successively proceeded by two sets of three Cd^{2+} ion incorporations [18]. Second, the coincidence of the Cys content and the Cys-to-Cd ratio of HpCdMT (18 Cys, 3:1 Cd-to-Cys ratio) with those of several crustacean MTs for which NMR structures are available (*Homarus americanus* MT, Protein Data Bank ID 1J5M [36], and *Callinectes sapidus* MT, Protein Data Bank IDs 1DMC, 1DMD, 1DME, and 1DMF [37]) clearly supports two separate moieties (with nine Cys each) folded into two separate domains. Finally, and as for mammalian MTs, there is no direct or indirect evidence of a bidominial or monodominial structure for the Cu_{12}–HpCuMT complex.

The HpMT system, namely, its two highly specific forms, HpCdMT and HpCuMT, has offered once again an optimum model to study the metal–protein specificity, this time to evaluate the differential coordination behavior of MT polypeptides with regard to either cognate or noncognate metal ions. As a conclusion, we demonstrate that when an MT binds its cognate metal, it yields well-folded complexes of limited stoichiometry, which should represent minimal-energy conformations. Instead, the incorporation of noncognate metal ions is better attributed to an unspecific reaction of the cysteinic thiolate groups with the metal ions, which is dependent on their concentration in the surrounding milieu, where no minimal-energy structure is reached, and where the MT peptide acts as a multidentate ligand that will bind metal ions until its capacity has been saturated.

Acknowledgments This work was supported by the Spanish Ministerio de Economía y Competitividad, (grants BIO2012-39682-C02-01 and BIO2012-39682-C02-02 to S.A. and M.C., respectively; these grants were partially supported by FEDER funding) and by the Austrian Science Foundation (grant P 23635-B20) to R.D. The authors from Barcelona are members of the 2009SGR-1457 Grup de Recerca de la Generalitat de Catalunya. The Spanish and Austrian groups were also financed by Acciones Integradas grants HU2006-0027 (Spain) and ES 02/2007 (Austria). S.P.R. received a predoctoral fellowship from the Departament de Química, Universitat Autònoma de Barcelona. We thank the Centres Científics i Tecnològics de la Universitat de Barcelona (ICP-AES, DNA sequencing) and the Servei d'Anàlisi Química de la Universitat Autònoma de Barcelona (CD spectroscopy, UV–vis spectroscopy, ESI-MS) for allocating instrument time.

References

1. Capdevila M, Bofill R, Palacios O, Atrian S (2012) Coord Chem Rev 256:46–52
2. Palacios O, Atrian S, Capdevila M (2011) J Biol Inorg Chem 16:991–1009
3. Capdevila M, Atrian S (2011) J Biol Inorg Chem 16:977–989
4. Dallinger R, Berger B, Hunziker PE, Kägi JHR (1997) Nature 388:237–238
5. Palacios O, Pagani A, Pérez-Rafael S, Egg M, Höckner M, Brandstätter A, Capdevila M, Atrian S, Dallinger R (2011) BMC Biol 9:4
6. Chabicovsky M, Klepal W, Dallinger R (2004) Environ Toxicol Chem 23:648–655
7. Chabicovsky M, Niederstaetter H, Thaler R, Hödl E, Parson W, Rossmanith W, Dallinger R (2003) Toxicol Appl Pharmacol 190:25–36
8. Dallinger R, Chabicovsky M, Hödl E, Prem C, Hunziker P, Manzl C (2005) Am J Physiol 289:R1185–R1195
9. Höckner M, Stefanon K, DeVaufleury A, Monteiro F, Perez-Rafael S, Palacios O, Capdevila M, Atrian S, Dallinger R (2011) Biometals 24:1079–1092
10. Pérez-Rafael S, Pagani A, Palacios O, Dallinger R, Capdevila M, Atrian S (2013) Z Anorg Allg Chem 639:1356–1360
11. Bongers J, Walton CD, Richardson DE, Bell JU (1988) Anal Chem 60:2683–2686
12. Capdevila M, Domènech J, Pagani A, Tío L, Villarreal L, Atrian S (2005) Angew Chem Int Ed 44:4618–4622
13. Capdevila M, Cols N, Romero-Isart N, Gonzalez-Duarte R, Atrian S, Gonzalez-Duarte P (1997) Cell Mol Life Sci 53:681–688
14. Bofill R, Palacios O, Capdevila M, Cols N, Gonzalez-Duarte R, Atrian S, Gonzalez-Duarte P (1999) J Inorg Biochem 73:57–64
15. Domenech J, Orihuela R, Mir G, Molinas M, Atrian S, Capdevila M (2007) J Biol Inorg Chem 12:867–882
16. Fabris D, Zaia J, Hathout Y, Fenselau C (1996) J Am Chem Soc 118:12242–12243
17. Bofill R, Capdevila M, Atrian S (2009) Metallomics 1:229–234
18. Dallinger R, Wang Y, Berger B, Mackay EA, Kägi JHR (2001) Eur J Biochem 268:4126–4133
19. Orihuela R, Monteiro F, Pagani A, Capdevila M, Atrian S (2010) Chem Eur J 16:12363–12372
20. Cols N, Romero-Isart N, Capdevila M, Oliva B, Gonzàlez-Duarte P, Gonzàlez-Duarte R, Atrian S (1997) J Inorg Biochem 68:157–166
21. Polec-Pawlac K, Palacios O, Capdevila M, Gonzalez-Duarte P, Lobinski R (2002) Talanta 57:1011–1017
22. Orihuela R, Domènech J, Bofill R, You C, Mackay EA, Kägi JHR, Capdevila M, Atrian S (2008) J Biol Inorg Chem 13:801–812
23. Pagani A, Villarreal L, Capdevila M, Atrian S (2007) Mol Microbiol 63:256–269
24. Gehrig PM, You C, Dallinger R, Gruber C, Brouwer M, Kägi JHR, Hunziker PE (2000) Protein Sci 9:395–402
25. Ding C, Festa RA, Chen YL, Espart A, Palacios O, Espin J, Capdevila M, Atrian S, Heitman J, Thiele D (2013) Cell Host Microbe 13:265–276

26. Pérez-Rafael S, Mezger A, Lieb B, Dallinger R, Capdevila M, Palacios O, Atrian S (2012) J Inorg Biochem 108:84–90
27. Pérez-Rafael S, Kurz A, Guirola M, Capdevila M, Palacios O, Atrian S (2012) Metallomics 4:342–349
28. Bofill R, Capdevila M, Cols N, Atrian S, Gonzàlez-Duarte P (2001) J Biol Inorg Chem 6:405–417
29. Artells E, Palacios O, Capdevila M, Atrian S (2013) Metallomics 5:1397–1410
30. Bofill R, Orihuela R, Romagosa M, Domenech J, Atrian S, Capdevila M (2009) FEBS J 276:7040–7056
31. Valls M, Bofill R, Romero-Isart N, Gonzalez-Duarte R, Abian J, Carrascal M, Gonzalez-Duarte P, Atrian S (2000) FEBS Lett 533:189–194
32. Palacios O, Espart A, Espin J, Ding C, Thiele D, Atrian S, Capdevila M (2014) Metallomics. doi:10.1039/C3MT00266G
33. Capdevila M, Palacios O, Atrian S (2010) Bioinorg Chem Appl. doi:10.1155/2010/541829
34. Zamyatin AA (1972) Prog Biophys Mol Biol 24:107–123
35. Hasler DW, Jensen LT, Zerbe O, Winge DR, Vasak M (2000) Biochemistry 39:14567–14575
36. Muñoz A, Forsterling FH, Shaw CF III, Petering DH (2002) J Biol Inorg Chem 7:713–724
37. Narula S, Brouwer M, Hua Y, Armitage IM (1995) Biochemistry 34:620–631